J. Fluid Mech. (1973), *vol.* 59, *part* 1, *pp.* 47–64
Printed in Great Britain

Finite amplitude sideways diffusive convection

By J. E. HART
Department of Astro-Geophysics, University of Colorado, Boulder

(Received 20 June 1972)

We consider the flow in a differentially heated vertical slot filled with a stably stratified solution. The stability of the flow driven by the differential heating is investigated in the limits of small but finite amplitude disturbances and very large solute Rayleigh number $R_S = g\beta(\partial S_a/\partial z)\, D^4/K_S\nu$. If the Schmidt number $H = K_T/K_S$ is of order 1, the growth of an initial perturbation at the neutral point is balanced by horizontal advection of solute and heat, and a steady equilibration amplitude is attained. The Nusselt number is independent of all fluid properties and is directly proportional to the Rayleigh number excess $\epsilon = (R_a - R_{ac})/R_{ac}$. If H is much greater than $|R_S|^{\frac{1}{3}}$, or if the disturbance wavenumber is slightly less than the critical wavenumber, subcritical instabilities are possible. In particular a resonant instability is possible. These theoretical predictions are consistent with previous experimental results and with the laboratory results described in this paper. In the experiments we find that the mixing of the initial sugar gradient is accomplished by convection cells which undergo transitions to larger wavelengths. The breakdown of the interfaces between convection cells is described.

1. Introduction

Several authors have previously considered the stability of flows with both horizontal and vertical mean temperature and salinity gradients. The motivation for these studies came partly from observations of layer formation in stably salt-stratified fluids prepared in the laboratory, often for unrelated purposes (see Turner & Stommel 1964). In such experiments a linearly stratified salt solution is subject (intentionally or accidentally) to side-wall heating. This creates vertical isotherms and slanted isohalines in the fluid which in certain circumstances can balance so that there are no horizontal density gradients. If one displaces a parcel of fluid sideways through these heat/salt gradients buoyancy forces will not normally act to create perturbation vorticity; except that if the diffusivities of salt and heat are unequal the density balance will be destroyed by differential diffusion. The motion resulting from this diffusive destabilization has been called sideways diffusive convection.

Various linearized stability problems concerned with the onset of this kind of diffusive convection have appeared in the literature. Blumsack (1967), Thorpe, Hutt & Soulsby (1969) and Hart (1971) have considered the stability of the motion generated in a differentially heated vertical slot filled with a linearly stratified salt solution. Another problem concerned with overturning in a rotating stratified

fluid (where angular momentum is analogous to salt) has been treated by McIntyre (1970) and some qualitatively supporting experiments were reported by Baker (1971). The stability of a binary mixture in a thermal diffusion column was discussed by Nikolaev & Tubin (1971), but in their calculation they apparently did not take large enough concentration gradients to allow for the sideways diffusive mode of instability.

The thermohaline problem mentioned above is the topic of this paper. It is of particular fundamental interest because it is an example of double diffusive convection where the analytical theory can cope with the experimental boundary conditions. Most of the theoretical studies (Stern 1960; Baines & Gill 1969; Veronis 1968; McIntyre 1970) employ constant temperature and salinity boundary conditions or work in an infinite region, so these problems are not easily simulated experimentally. Also, in view of the existence of a wide range of analogous problems with applications in aspects of rotating geophysical fluid dynamics, oceanography and chemical engineering, results from the thermohaline (or thermosolutal) problem are of particular interest, especially since this system offers an opportunity to study a kind of double diffusive convection both theoretically and in the laboratory. In this paper we shall be concerned with flows in a narrow, very tall channel. Wirtz, Briggs & Chen (1972) and Chen, Briggs & Wirtz (1971) have studied certain aspects of wide-channel flows in the laboratory and have made some numerical integrations. These wide-gap flows have time-dependent basic states and boundary conditions which are quite different from those reported here, and while some of the physics may be similar, quantitative comparisons between the two cases cannot be made at this time.

The author (Hart 1971, hereafter called I) compared numerical and asymptotic linear stability results with the experimental results of Thorpe, Hutt & Soulsby (1969), whose report will be called THS. Their experiments were run in a narrow vertical slot, with walls maintained at a temperature difference ΔT. The slot was very tall and initially contained a constant vertical gradient of salt $\partial S_a/\partial z$. The differential heating generated a parallel mean flow near the centre of the apparatus which was observed to become unstable at a critical value of the thermal Rayleigh number $R_a = g\alpha\Delta T D^3/K_T\nu$ which was a function of the salinity Rayleigh number $R_S = g\beta(\partial S_a/\partial z)\, D^4/K_S\nu$.

In comparing the linear theory and these experiments it was found in I that both the numerical and the asymptotic theory overestimate the critical Rayleigh number R_a at large values of $-R_S$. Also THS reported that all cells appeared to rotate in the same sense with a wavelength twice that predicted by linear theory. We shall see that this was a consequence of comparing an interior theory with observations made in the side-wall boundary layers. Nonetheless the corrected experimental wavenumber results of THS shown in figure 6(*c*) are lower than the predicted values. Now it is possible that these discrepancies are due to non-Boussinesq effects or to violation of quasi-static assumptions used in the theory, but without a more complicated calculation we can only speculate (see I) that these explanations are incorrect. Another possibility is a subcritical finite amplitude instability which might develop at large $(-R_S)$ when the mean

velocity field effectively vanishes. The testing of this hypothesis is the main motivation for this study.

To help in the effort to discover what could account for the above-mentioned discrepancies we have conducted more experiments with a more sensitive visualization method. Weak sinusoidal circulations with wavenumbers near but below the predicted wavenumbers do appear at onset but last only a very short time, as the experimental system makes a series of transitions to lower wavenumbers. The transitions to fewer and fewer cells is apparently the way the initial solute gradient is mixed up, and the final state of a single cell just corresponds to the thermally driven flow in the box.

The substance of this paper is divided into the following parts. In § 2 we review the analytic linear theory based on an expansion of the equations in terms of the small parameter $-R_S^{-\frac{1}{6}}$. A finite amplitude expansion is constructed based upon a small parameter $\epsilon = (R_a - R_{ac})/R_{ac}$, where R_{ac} is the critical Rayleigh number obtained from linear theory. In § 3 the various sequential problems in the double-parameter ($|\epsilon|^{\frac{1}{2}}$, $|R_S|^{-\frac{1}{6}}$) expansion are solved to $O(|\epsilon|)$, and an existence condition on the $O(|\epsilon|^{\frac{3}{2}})$ problem shows that the amplitude $A(t)$ of the fundamental disturbance satisfies an equation of the form

$$\dot{A} - a_0 A + a_1 |A|^2 A = 0.$$

The Landau constants are evaluated for $H \sim 1$ and $H > |R_S|^{\frac{1}{6}}$. Section 4 describes the experimental results. Conclusions and a summary are given in § 5.

2. The linear theory

The formulation of the governing equations is the same as that in I. We assume that the channel is infinitely tall, differentially heated at the sides, and filled with a vertical S-stratified liquid.† The geometry and boundary conditions are shown in figure 1. Within the Boussinesq approximation the non-dimensional equations are

$$P_r^{-1}\frac{\partial \mathbf{u}}{\partial t} + \frac{R_a}{P_r}\mathbf{u}.\nabla\mathbf{u} = -\nabla p + (T-S)\hat{\mathbf{z}} + \nabla^2\mathbf{u}, \tag{2.1}$$

$$\partial T/\partial t + R_a \mathbf{u}.\nabla T = \nabla^2 T, \tag{2.2}$$

$$H\,\partial S/\partial t + H R_a \mathbf{u}.\nabla S + R_S w = \nabla^2 S, \tag{2.3}$$

$$\nabla.\mathbf{u} = 0. \tag{2.4}$$

The thermal Rayleigh number mentioned above is defined by

$$R_a \equiv g\alpha \Delta T D^3/K_T \nu,$$

and

$$R_S = g\beta \frac{\partial S_a}{\partial z} D^4/K_S \nu \ll 0.$$

We have specified a stable stratification ($R_S < 0$) and without loss of generality we choose $R_a > 0$. The Prandtl number $P_r = \nu/K_T$ and the Schmidt number $H = K_T/K_S$. Velocities have been scaled by $g\alpha \Delta T D^2/\nu$, lengths by D, temperature

† S will denote a general solute, which was either sugar or salt in the experiment.

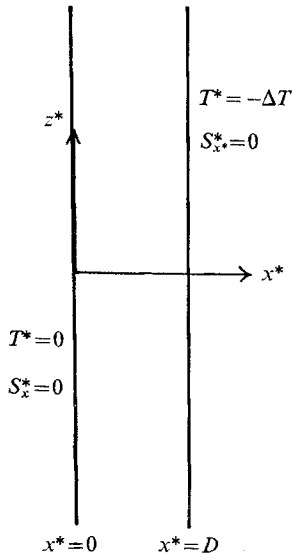

FIGURE 1. Geometry and boundary conditions for the problem. In the experiments the box is of finite depth and height but this seems to have little effect except in the very final stages of development. The box initially contains a linearly stratified solute: $\partial S_a/\partial z$ = constant.

by ΔT, solute concentration by $\alpha\Delta T/\beta$ and time by K_T/D^2. The other dimensional constants are α, the coefficient of thermal expansion, β, the coefficient of volumetric expansion, K_T, the diffusivity of temperature, K_S, the diffusivity of solute, ν, the kinematic viscosity, and g, the gravitational acceleration.

The boundary conditions at $x = 0, 1$ are

$$T = 0, -1, \quad S_x = 0, \quad \mathbf{u} = 0. \qquad (2.5), (2.6), (2.7)$$

With side walls impermeable to solute any convective overturning would tend to destroy the basic vertical salinity gradient $\partial S_a/\partial z$ were it not for compensating vertical advection of new salty (fresh) fluid. As we shall see, this is accomplished by narrow vertical boundary currents near $x = 0$ and $x = 1$.

As was discussed in I the thermal forcing will drive a parallel flow in the channel This will be governed by the equations

$$w_{0xx} + T_0 - S_0 = 0, \qquad (2.8)$$

$$T_{0xx} = 0, \quad S_{0xx} - R_S w_0 = 0. \qquad (2.9), (2.10)$$

The solutions for large $-R_S$ are

$$T_0 = -x, \qquad (2.11)$$

$$w_0 = \frac{+e^{-mx}\sin mx}{2m^3} + (1), \quad S_0 = -x - \frac{e^{-mx}\cos mx}{m} + (1), \qquad (2.12), (2.13)$$

where the (1) terms contain similar boundary layers near $x = 1$. The inverse boundary-layer thickness is

$$m = (-\tfrac{1}{4}R_S)^{\frac{1}{4}}. \qquad (2.14)$$

In I it was found that the linearized stability problem for large $-R_S$ could be split up into interior and boundary components. In addition the strong vertical stabilization forced the disturbances into thin layers in which $\partial/\partial z \gg \partial/\partial x$ in the interior. In this paper we want to consider finite amplitude effects in addition and to do this we shall consider a perturbation solution off the linear neutral curve given by

$$R_{ac} = R_{ac}(-R_S, k, P_r, H)$$

by an amount ϵ. That is we consider

$$R_a = R_{ac} + \epsilon R_{ac}. \tag{2.15}$$

In this section on the linear problem we shall just note that a consistent expansion of the nonlinear one-wave problem requires that we expand variables in powers of $|\epsilon|^{\frac{1}{2}}$. Taking the large value of $-R_S$ and the small value of ϵ into consideration we are motivated to expand the stream function

$$\Psi(w = \Psi_x, u = -\Psi_z)$$

as
$$\Psi = \Psi_0 + \sum_{i=1}^{\infty}\sum_{j=0}^{\infty} |\epsilon|^{\frac{1}{2}i} |R_S|^{-\frac{1}{6}j} (\Psi_{ij}(z, x, t) + \tilde{\Psi}_{ij}(|R_S|^{+\frac{1}{4}} x, z, t)), \tag{2.16}$$

with similar expansions for T and S. We seek solutions which satisfy

$$\Psi = \Psi_x = S_x = T = 0 \quad \text{at} \quad x = 0, 1.$$

The parameter setting $i = 1, j = 0$ generates the linear stability equations from (2.1)–(2.4). As the equations are linear with coefficients depending at most on x we can look for solutions $\Psi_{10} = \psi_{10}(x)\, e^{\omega t}\, e^{ikz}$, etc., where k is implicitly assumed to be of $O(|R_S|^{\frac{1}{6}})$. Then we find:

$$P_r^{-1}\omega k^2 \psi_{10} + k^4 \psi_{10} + dT_{10} - dS_{10} = 0, \tag{2.17}$$

$$-ikR_a \psi_{10} - \omega T_{10} - k^2 T_{10} = 0, \tag{2.18}$$

$$-ikHR_a \psi_{10} - d\psi_{10} R_S - H\omega S_{10} - k^2 S_{10} = 0, \tag{2.19}$$

$$-P_r^{-1}\omega |R_S|^{\frac{1}{2}} d^2 \tilde{\psi}_{10} + |R_S|\, d^4 \tilde{\psi}_{10} + |R_S|^{\frac{1}{4}} (d\tilde{T}_{10} - d\tilde{S}_{10}) = 0, \tag{2.20}$$

$$-\omega \tilde{T}_{10} + |R_S|^{\frac{1}{2}} d^2 \tilde{T}_{10} = 0, \tag{2.21}$$

$$-H\omega \tilde{S}_{10} + |R_S|^{\frac{1}{2}} d^2 \tilde{S}_{10} - |R_S|^{\frac{1}{4}} \tilde{\psi}_{10} = 0, \tag{2.22}$$

where $d = d/dx$. The advection terms in (2.20)–(2.22) are omitted because they are of higher order in $|R_S|^{-\frac{1}{6}}$. There are also two purely diffusive side-wall boundary-layer solutions of the $|\epsilon|^{\frac{1}{2}}$ equations which are needed to help satisfy boundary conditions. These are

$$T_{10d} = a_7\, e^{k(x-1)} + a_8\, e^{-kx} \tag{2.23}$$

and
$$S_{10d} = a_7\, e^{k(x-1)} + a_8\, e^{-kx}. \tag{2.24}$$

In I it was noted that the boundary layers described by (2.20)–(2.24) were steady ($\omega \ll |R_S|^{\frac{1}{2}}$) and that they dominated the differentiated boundary conditions $w = d\psi = 0$ at $x = 0, 1$, and $dS = 0$ at $x = 0, 1$. This can be seen by writing down the boundary conditions at $x = 1$, putting in the two boundary solutions at this

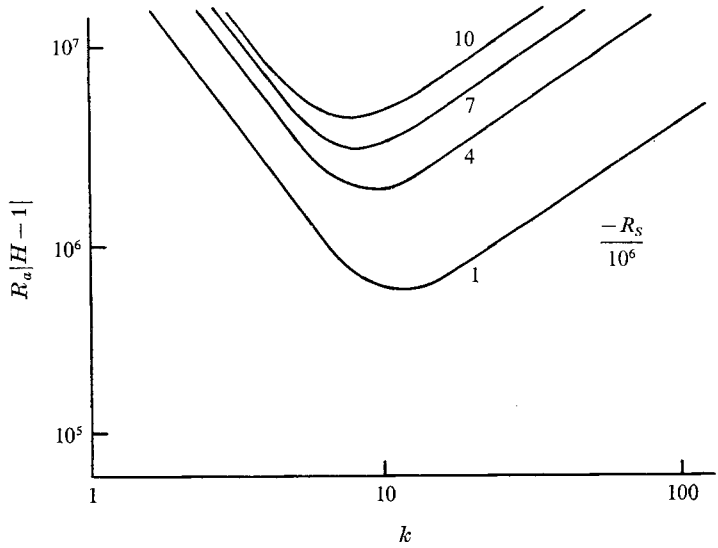

FIGURE 2. Curves of neutral stability determined from the lowest order linear interior theory.

wall, and by using simple algebra to show that we can satisfy all the boundary conditions to $O(|R_S|^{-\frac{1}{3}})$ provided we take $\psi_{10}|_{x=1} = 0$. Similar considerations hold at $x = 0$. Thus

$$\psi_{i0} = 0 \quad \text{at} \quad x = 0, 1 \tag{2.25}$$

is the proper boundary condition for the interior problem. This boundary condition applies to all orders of the nonlinear expansion bracketed between the linear problem and the first diffusive ($j = 1$) correction.

The assumption that $\omega \ll |R_S|^{\frac{1}{2}}$, verified below, enables us to find ω from the solution of the interior equations, subject to (2.25). From this we find the eigenvalue equation

$$k^6 R_a^2(1-H)^2 + 4R_S(\omega k^2/P_r + k^4)(\omega + k^2)^2(H\omega + k^2) = 4n^2\pi^2 R_S^2(\omega + k^2)^2, \tag{2.26}$$

where n is an integer. If we write $\omega = \omega_r + i\omega_i$ and equate imaginary parts of the above equation, we find

$$\frac{-2k^8 R_a^2(H-1)^2\omega_i}{[(\omega_r + k^2)^2 - \omega_i^2]^2 + 4k^2\omega_i^2} = -4R_S\omega_i[2H\omega_r P_r^{-1} + (H + P_r^{-1})k^2].$$

Thus, if $\omega_r > 0$ (growing solutions), we must have $\omega_i = 0$. Overstability is not possible and ω must be real. The neutral curve is found to be at

$$R_{ac}^2(H-1)^2 = 4n^2\pi^2 k^{-2} R_S^2 - 4k^4 R_S, \tag{2.27}$$

with a minimum at

$$k_c = (-\tfrac{1}{2}n^2\pi^2 R_S)^{\frac{1}{6}} \tag{2.28}$$

such that the most unstable mode occurs at

$$R_{ac} = 2^{\frac{1}{3}} 6^{\frac{1}{2}} |R_S|^{\frac{5}{6}} (n\pi)^{\frac{2}{3}} / |H-1|. \tag{2.29}$$

Figure 2 shows a set of neutral curves for various R_S.

The solution for ψ_{10} under neutral conditions is

$$\psi_{10} = A(e^{r_1 x} - e^{r_2 x})\, e^{ikz} + *,$$

where $*$ denotes the complex conjugate of the part given. The characteristic exponents are

$$r_{2,1} = -\frac{ikR_{ac}(H-1)}{2R_S} \pm \frac{1}{2R_S}(-k^2R_a^2(H-1)^2 - 4R_S k^6)^{\frac{1}{2}}. \tag{2.30}$$

If $R_a = R_{ac} + \epsilon R_{ac}$ we can assume $\omega = O(\epsilon)$ and obtain, for large P_r,

$$\omega = \frac{R_{ac}k^2 \operatorname{sgn}\epsilon}{R_{ac} + 2R_S k^4 H/R_{ac}(H-1)^2} = \frac{|R_S|^{\frac{1}{3}}(n^2\pi^2)^{\frac{1}{3}}}{2^{\frac{1}{3}}(1+\frac{1}{6}H)} \text{ at the critical point.} \tag{2.31}$$

It is seen that the growth rate increases with $-R_S$, decreases with increasing H, and is of order $k^2 \sim |R_S|^{\frac{1}{3}} \ll |R_S|^{\frac{1}{2}}$, as assumed. If $\epsilon < 0$ the linear growth rate of course becomes a damping rate.

3. Finite amplitude effects

We wish to consider finite amplitude corrections to the basic solution. We assume here that only one fundamental wave is present. We want the nonlinear effects to be more important than boundary and interior corrections which, if anything, caused increased disparity between experiment and theory. Thus we must take ϵ large enough so that nonlinear terms dominate; that is $|\epsilon| > |R_S|^{-\frac{1}{6}}$. Since we have defined ϵ by (2.15), equation (2.31) suggests that we introduce a new time scale $\tau = \epsilon t$ so that $\partial/\partial t \to \epsilon\, \partial/\partial\tau$. Recall that the $O(|\epsilon|^{\frac{1}{2}})$ solutions on the neutral curve were

$$\psi_1 = A(\tau)\,(e^{r_1 x} - e^{r_2 x})\, e^{ikz} + *, \quad T_1 = -iR_{ac}k^{-1}\psi_1, \quad S_1 = T_1 + k^4 \int \psi_1 dx, \tag{3.1}$$

where we have dropped the second subscript, since $j = 0$ in all that follows. The $O(\epsilon)$ interior equations consist of those describing the mean-field corrections,

$$\bar{w}_{2xx} + \bar{T}_2 - \bar{S}_2 = \frac{R_{ac}}{P_r}\overline{(\psi_{1x}\psi_{1xz} - \psi_{1z}\psi_{1xx})} = -\frac{8n^2\pi^2 R_{ac}k|A|^2}{P_r}\sin 2n\pi x, \tag{3.2}$$

$$\bar{T}_{2xx} = R_{ac}\overline{(\psi_{1x}T_{1z} - \psi_{1z}T_{1x})} = 8R_{ac}^2 n\pi |A|^2 \sin 2n\pi x, \tag{3.3}$$

$$\bar{S}_{2xx} - R_S\bar{w}_2 = 4H(H+1)R_{ac}^2 n\pi |A|^2 \sin 2n\pi x, \tag{3.4}$$

along with equations for the parts dependent on e^{2ikz},

$$16k^4\psi_2 + dT_2 - dS_2 = 0, \tag{3.5}$$

$$-4k^2T_2 - 2ikR_{ac}\psi_2 = 0, \tag{3.6}$$

$$-4k^2S_2 - 2ikR_{ac}H\psi_2 - R_S d\psi_2 = -ik^5\frac{(r_2-r_1)^2}{r_1 r_2}HR_{ac}A^2 e^{(r_1+r_2)x} + *. \tag{3.7}$$

The bar denotes the z average over one basic period $2\pi/k$. Note that as opposed to the weakly nonlinear theory for ordinary thermal convection between horizontal plates, here we force a response proportional to e^{2ikz}. This comes about because the fundamental cells are tilted and influenced by boundaries. Physically it

describes the modification to the initial vertical salt gradient. The solutions for the mean corrections are

$$\overline{w}_2 = \frac{4n\pi(H^2-1)\,R_{ac}^2|A|^2\sin 2n\pi x}{16n^4\pi^4 - R_S}, \tag{3.8}$$

$$\overline{T}_2 = -2R_{ac}^2|A|^2\sin 2n\pi x/n\pi, \tag{3.9}$$

$$\overline{S}_2 = \left[-2R_{ac}^2|A|^2/n\pi - \frac{4n^3\pi^3(H^2-1)\,R_{ac}^2}{16n^4\pi^4 - R_S}\right]|A|^2\sin 2n\pi x \tag{3.10}$$

$$\sim |R_S|^{\frac{10}{6}}|A|^2/H^2.$$

The heat and solute advection by the disturbances cause corrections to the horizontal parts of the mean fields which reduce the horizontal driving for the perturbations (note that the coefficients of T_2 and S_2 are < 0).

The z-dependent response is

$$\psi_2 = (d_2\,e^{(r_1+r_2)x} + d_3\,e^{p_3 x} + d_4\,e^{p_4 x})\,A^2\,e^{2ikz} + *, \tag{3.11}$$

where the second and third terms on the right-hand side represent complementary solutions of (3.5)–(3.7) and are needed to satisfy $\psi_2(x = 0, 1) = 0$. Now

$$d_2 = \frac{-4n^2\pi^2H(H-1)\,R_{ac}^2}{-4n^2\pi^2R_S - 60k^6} \sim |R_S|^{\frac{4}{6}} \tag{3.12}$$

and the other parameters are easily obtained from (3.5)–(3.7) and by applying boundary conditions. Note that d_3, d_4, P_3 and P_4 will in general be complex and $d_3, d_4 \sim d_2$.

The $O(|\epsilon|^{\frac{3}{2}})$ problem is

$$\begin{aligned}\mathscr{L}(\psi_3) = {} & HS_{1x\tau} - T_{1x\tau} + R_{ac}(1-H)\,\psi_{1xz} \\ & - R_{ac}P_r^{-1}(\psi_{1x}\psi_{2zzz} - \psi_{1z}\psi_{2xzz} + \psi_{2x}\psi_{1zzz} - \psi_{2z}\psi_{1xzz})_{zz} \\ & - R_{ac}(\overline{w}_2 T_{1z} + \psi_{1x}T_{2z} + \psi_{2x}T_{1z} - \psi_{1z}T_{2x} - \psi_{2z}T_{1x} - \psi_{1z}\overline{T}_{2x})_x \\ & + HR_{ac}(\overline{w}_2 S_{1z} + \psi_{1x}S_{2z} + \psi_{2x}S_{1z} - \psi_{1z}S_{2x} - \psi_{2z}S_{1x} - \psi_{1z}\overline{S}_{2x})_x \\ = {} & f_1\,e^{ikz} + f_2\,e^{3ikz} + *.\end{aligned} \tag{3.13}$$

$\mathscr{L}$ is the operator of the linear problem if we isolate the e^{ikz} part of the problem. Thus a solution exists only if

$$\int_0^1 \hat{\psi}_1 f_1(x,\tau)\,dx = 0, \tag{3.14}$$

where $\hat{\psi}_1$ is the solution of the adjoint problem

$$-R_S\,d^2\hat{\psi}_1 + ik(H-1)\,R_{ac}\,d\hat{\psi}_1 - k^6\hat{\psi}_1 = 0, \quad \hat{\psi}_1(x = 0, 1) = 0. \tag{3.15}$$

The almost trivial solution of (3.15) and the application of the existence condition (3.14) will yield the amplitude equation for A. The latter task is anything but trivial since essentially all of the terms on the right-hand side of (3.13) contribute to f_1. Now if $H = O(1)$ it can be seen that except for a certain special instance discussed below the mean-field corrections will dominate the e^{2ikz} terms (compare (3.12) with (3.10)). On the other hand, if $H \geqslant |R_S|^{\frac{1}{6}}$, it is somewhat

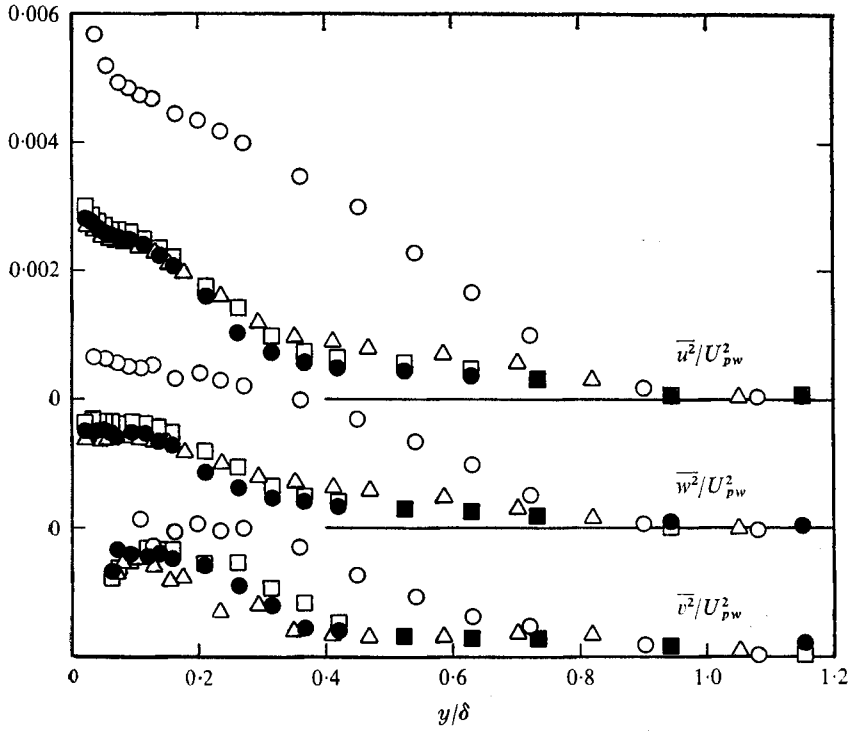

FIGURE 12. Distribution of $\overline{u^2}/U_{pw}^2$, $\overline{v^2}/U_{pw}^2$ and $\overline{w^2}/U_{pw}^2$ across the boundary layer. ○, $x = 24$ in.; △, $x = 59$ in.; □, $x = 67$ in.; ●, $x = 71$ in.

5. Discussion

The wall friction data obtained by the Clauser plots are in agreement with an overall momentum balance described in appendix A, but appear a bit large relative to a wall extrapolation of the hot-wire data in figure 11. However, Bissonnette & Mellor (1971) had previously determined that $-\overline{uv}$ (but not the energy component) data are measured low by the present system roughly when $y/l \lesssim 2$, where l is the wire length. This corresponds to $y/\delta \lesssim 0{\cdot}13$ in figure 11.

Further evidence that curvature does not affect the flow near the wall is contained in figures 13(*b*) and 15, where the turbulent energy and production normalized by u_τ are similar to the flat-plate data in the wall region

$$(y < 0{\cdot}16\delta \cong 200\nu/u_\tau).$$

The data at $x = 59$ in. (figure 13*b*) are influenced by the favourable pressure gradient at the entrance to the curved section; however, this influence disappears by the time the flow reaches $x = 67$ in.

Equilibrium was not achieved. This is due primarily to the curvature itself, which has literally 'turned off' the shear stress at $y \cong 0{\cdot}4\delta \cong 0{\cdot}4$ in., where the velocity gradient is substantial. The ratio Δ/R increases a bit but this is probably a minor influence. (Note that in figure 12 the scattered deviation of $\overline{uv}$ about zero when $y > 0{\cdot}4\delta$ is about the same as the deviation of $\overline{uw}$ everywhere. This can be taken as the measurement error for the system although agreement of

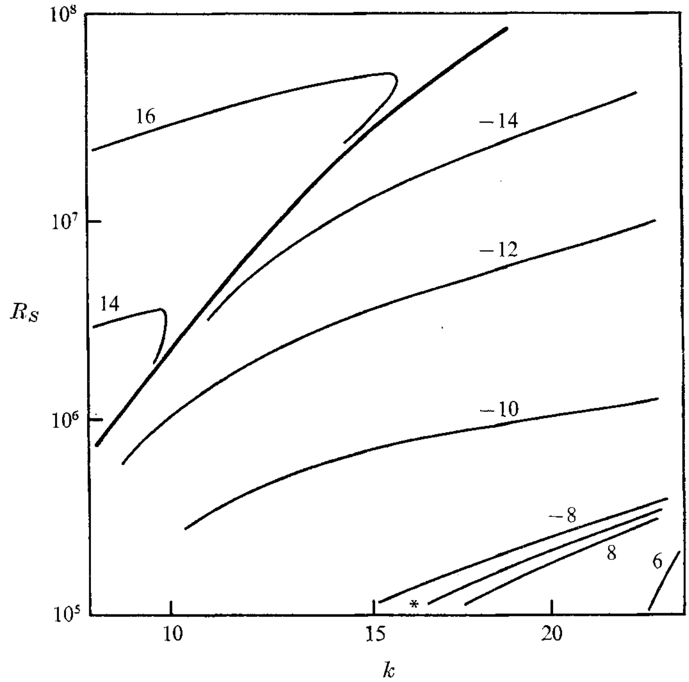

FIGURE 3. The function sgn $(2X+g+g^*)$ $|\log_{10}|2X+g+g^*||$ as a function of R_S and k for $H = 281$ (sugar, water).

I will not comment further on this since as we shall see below this equilibrium may not be attained for any H.

The most interesting theoretical results come when we evaluate g. In terms of the existence of possible finite amplitude subcritical instabilities what is important is the sign of $X+\frac{1}{2}(g+g^*)$. We can vary k along the neutral curve at fixed R_S and H and calculate this combination.† Figure 3 shows the results for $H = 281$. We have plotted $[\text{sgn}\{X+\frac{1}{2}(g+g^*)\}\,|\log|X+\frac{1}{2}(g+g^*)||]$ in order to compress large variations into the plot. Since this Landau constant is generally $\gg 1$ no ambiguity results.

It is seen that the Landau constant multiplying the nonlinear term of (3.22) can in general be negative for a range of k at each value of R_S. This means that subcritical instabilities are possible if the background perturbations are large enough. The range of k over which this finite amplitude instability is possible diminishes as H becomes of $O(1)$. This is consistent with the fact that the stabilizing part X (equation 3.19), which describes the effect of reducing the interior mean horizontal gradients by the fundamental, goes as $|R_S|^{\frac{16}{6}}/H^2$, while the destablizing part g (equation 3.21) goes as $|R_S|^{\frac{14}{6}}$.

Most interesting are the resonance lines along which g becomes infinite. Thus no matter how small H is we still will get a small region where $Re\,(X+g)$ is

† The usual justification of a one-wave analysis is that just inside the critical point only one wavenumber will grow. However, if subcritical instabilities are possible for any k the general normal-mode cascade method based on neutral solutions may be invalid, and this possibility must be checked.

negative. The source of this resonance can be seen to arise from the forcing of the second harmonic of the fundamental. From (3.12) it is seen that the response to this forcing, described by (3.5)–(3.7), becomes infinite when

$$k_r = (\tfrac{1}{15}n^2\pi^2|R_S|)^{\frac{1}{6}}, \tag{3.23}$$

or when

$$k_r \doteq 0{\cdot}715k_c. \tag{3.24}$$

For the certain k along the neutral curve given by (2.27) the second harmonic (e^{2ik_rz}) forces a resonant response in Ψ_2. It is interesting that the point $(R_{ac}, 2k_r)$ does not lie on the neutral curve on the other side of critical wavenumber k_c, where we might naturally expect a resonance, but outside it. This is because the x-dependent part of the forced eigenfunction is different from that of the neutral eigensolution. The singular behaviour arises from the particular dynamics of the system. The mixing of the stable vertical solute gradient by the disturbances destabilizes the system, and in particular wavenumbers near k_r are most efficient in doing this.

The resonance at k_r suggests that we consider *two* primary waves

$$A(\tau, x)\, e^{ik_rz} + *, \quad B(\tau, x)\, e^{2ik_rz} + *.$$

The solvability condition at the quadratic ($O(\epsilon)$) level requires that we add a faster time scale $\hat{\tau} = |\epsilon|^{\frac{1}{2}}t$ to balance nonlinearities. Then we shall find a nonlinear exchange of energy between A and B. There is as yet no coupling to the mean fields. This comes in at third order, and on the slower time scale. Since all the harmonics $(3, 4, -3, -4)$ generated in the $O(|\epsilon|)$ problem are important, the algebra required to compute the coefficients of the $O(|\epsilon|^{\frac{3}{2}})$ problem by using relations like (3.14) on the two forced equations will be abysmal and this analysis has not been attempted. We only note that the coefficients multiplying the nonlinear terms at quadratic level are large, so that energy transfers between modes occur very rapidly.

In conclusion, our theory has told us of the existence of subcritical finite amplitude instabilities at all values of $H > |R_S|^{\frac{1}{3}}$ (further calculation would probably extend the range to all H, provided the background perturbations were large enough). At $k_r = (\frac{1}{15}n^2\pi^2|R_S|)^{\frac{1}{6}}$ a resonant type of finite amplitude instability is possible wherein background perturbations in either k_r or $2k_r$ can grow. Further discussion of the physics involved will be given in § 5.

4. Experimental results

The theoretical conclusions of § 3 are in substantial agreement with the experiments of THS. This can be seen from figure 6(*c*) and figure 5(*a*) of I. The observation of onset Rayleigh numbers greater than critical for $-R_S < 10^6$ may well be a reflexion of boundary influences on the nonlinear interior dynamics (e.g. $|\epsilon| \leqslant |R_S|^{-\frac{1}{6}}$). In spite of this favourable comparison with existing experiments we decided to conduct some more experiments to check the theory further and to make observations of the long-time development of the sideways diffusive convection. Our apparatus is similar to theirs, a tall and narrow slot with conducting walls maintained at constant temperatures ($\pm 0{\cdot}01\,^\circ$C). The initial

solute (sugar) gradient was made with an 'Osterizer' (Oster 1965). The fluid was injected very slowly (at 1 cc/10 s) into the box (40 cm high × 1 cm wide × 18 cm deep) using a metered tubing pump to ensure a uniform gradient. The principal differences between our experiments and those of THS are the following.

(i) A larger height-to-width ratio (40 : 1).

(ii) The use of a sugar as a solute in most runs ($H_{\text{sugar}} \sim 2{\cdot}8 H_{\text{salt}}$).

(iii) The use of the thymol dye visualization technique (Baker 1966).

4.1. *Observations of the onset of disturbances*

The Rayleigh number was slowly increased (by varying ΔT) from $\frac{1}{2}R_{ac}$ to $\sim R_{ac}$ over a period of about 4–5 hours. Dye lines were induced along $x = 0$ at periodic intervals. Figure 4(*a*) (plate 1) shows a typical visualization of the onset of instability. Note that the instability initially appears in bursts (which is probably typical of subcritical instabilities). The disturbances fill the entire slot relatively quickly. Note that the interior flow has a $\sin kz$ type structure. Apparently the statement of THS about asymmetric cells of double wavelength is partly a result of their observations being made near the walls (by looking at dye coming off suspended potassium permanganate particles). It would appear that this is a consequence of the interior and boundary-layer nature of the flow. For example the theoretical solution

$$\psi = \frac{-e^{-m(1-x)}}{4m^4}[\cos m(1-x) + \sin m(1-x)] - A\, e^{ikz} \times \left[e^{r_1 x} - e^{r_2 x} + \frac{2in\pi}{m} e^{-m(1-x)} \sin m(1-x)\right]$$

shown in figure 5 exhibits a similar behaviour if A is small. A dye column injected next to the right-hand wall will enter the interior mostly at points equivalent to once every *two* rolls. But a column launched near $x = \frac{1}{2}$ will show the $\sin kz$ structure of the fundamental. The second harmonic will also cause a distortion away from the pure sinusoidal structure of the fundamental. This will also be strong near the walls (but outside the $-R_S^{\frac{1}{4}}$ layers). These effects are evident in figure 4(*b*) (plate 1).

Our measured values of the onset parameters are shown in figure 6. Most of the experiments were made at larger $-R_S$ than those run by THS. For some R_S two runs were made with nearly identical results for each run, although the initial bursts of wavelets occurred in different parts of the tank. The flows are subcritically unstable even for our most carefully run experiments. Again k is approximately k_r not k_c.† In addition there is a tremendous amount of hysteresis in the system. If R_a is decreased after the subcritical motions have set in, the disturbances do not disappear until R_a is halved.‡

At the first observation of wavelets the advance of ΔT was halted. In parts of the tank new bursts of waves would become visible so that one might have ex-

† At this time it is useful to point out that the length scale based on the stratification alone, $\alpha\Delta T/\beta S_{0z}$ (which predicts $k \sim 1{\cdot}35|R_S|^{\frac{1}{6}}$ for most of our data), overestimates k and does not really explain the observation of rolls at a critical temperature difference.

‡ The precise value of course depends on how long the disturbances have had to develop.

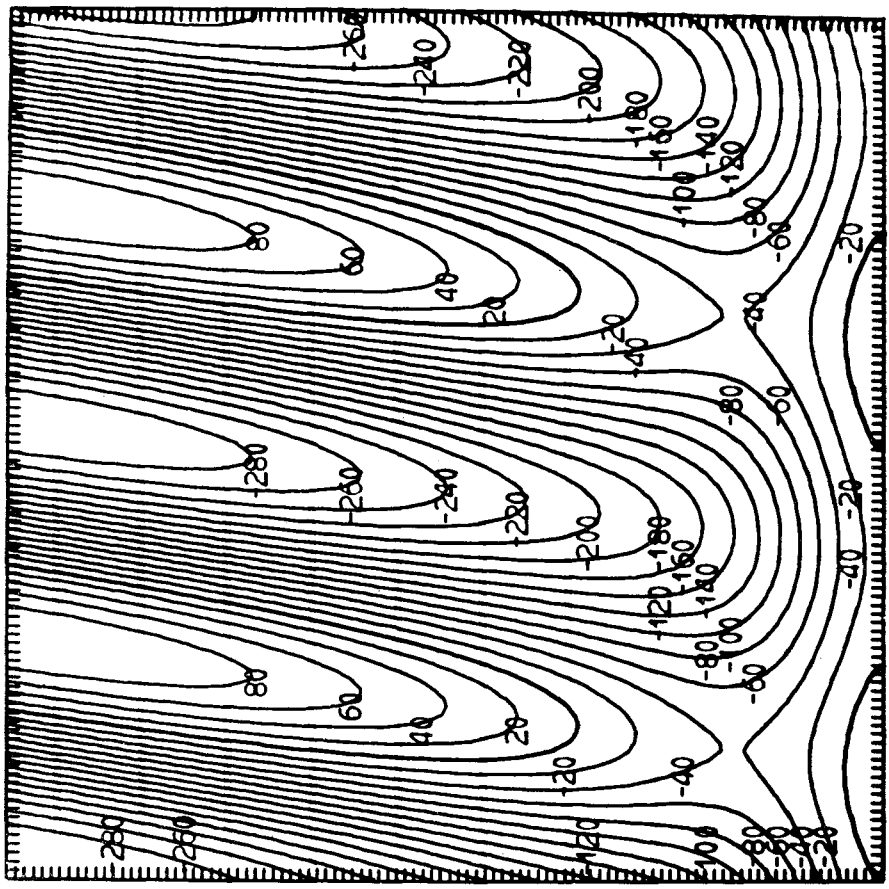

FIGURE 5. Theoretical streamline pattern of the combined interior and boundary-layer flow for $x \geqslant \frac{1}{2}$. $R_S = -10^6$ and $A = 10^{-6}$.

pected them to fill the slot. However, the first bursts to be observed, having grown to larger amplitudes, appeared to break down in a rather short time (5–10 min) into cells of roughly double the wavelength. Figures 4(*c*) and (*d*) (plate 1) show a typical development. It appears that the cells which started up first attain larger amplitudes than their neighbours and then can entrain them. This very weak amplitude process (the velocities are still small, of order 0·001 cm/s) probably indicates instability of the basic subcritical solution to perturbations of larger wavelengths.

4.2. *The development of the convecting system*

Over a long period of time (10–60 h) the system gradually attains a state of uniform concentration. The mixing of the initial solute gradient is done by the convection cells. At fixed ΔT, equal to that for which waves were first observed, transitions to larger and larger cell heights are observed. Figure 7 shows two typical experimental histories, t_0 being the time of first observation of waves. The transitions do not occur simultaneously over the slot because the initial perturbations are not uniform in amplitude; so the steps in figure 7 are not sharp.

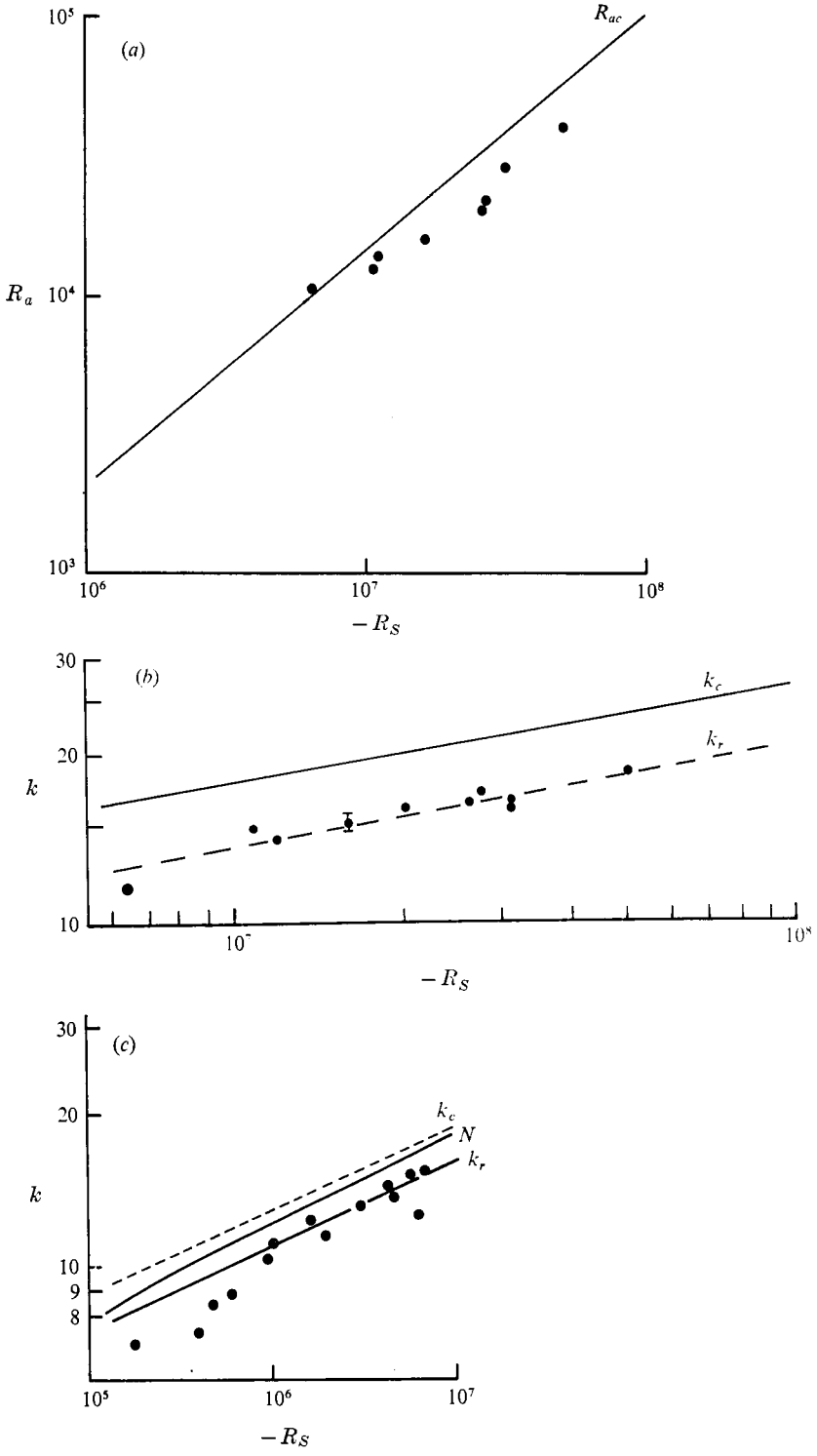

FIGURE 6. Onset parameters for our experiments with sugar and water. ——, predictions of linear theory; – – –, the resonant wavenumber. The data have been corrected for the change in the mean viscosity due to the sugar. In figure 6(*c*) we compare the numerical linear (N), analytic linear (k_c) and resonant nonlinear (k_r) theories with the experimental results of THS.

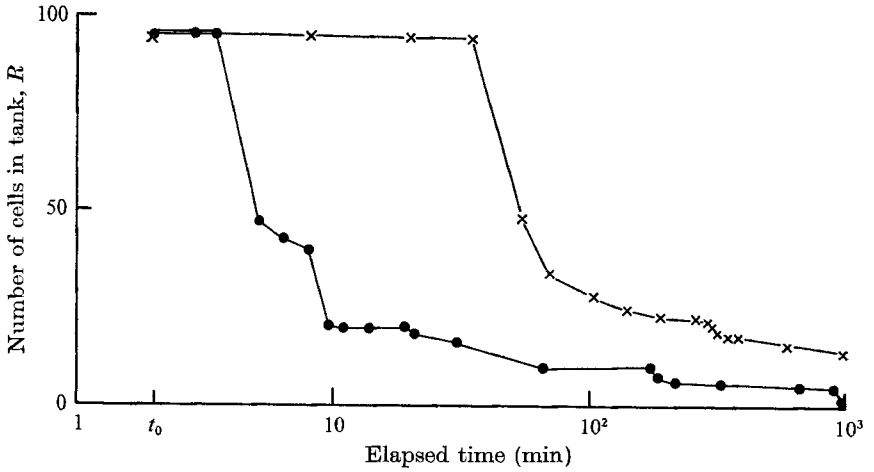

FIGURE 7. Time evolution of the system at two values of ΔT. ●, $\Delta T = 8{\cdot}5$ °C, $R_S = -2{\cdot}6 \times 10^7$; ×, $\Delta T = 1{\cdot}50$ °C, $R_S = -2{\cdot}0 \times 10^7$. In each case $H = 281$, $P_r \sim 6{\cdot}7$.

Figure 8 (plate 2) shows some dye-line observations of the cell evolution. Although the cells are initially sinusoidal in z, one can easily see the development of boundary-layer circulations in the cells.

The mechanism for early transitions appears to be a laminar wave selection process. At large ΔT or t, however, strong interfaces form between cells. As adjacent cells continuously mix up their own stabilizing solute gradients their upwards and downwards velocities increase. The stable interfaces which force these currents to turn become deformed until they are, as near as we can tell, statically unstable. At this time the interface breaks down in a shower of turbulence and 'salt' fingers, so that a cell with double wavelength is set up. Figure 9 (plate 3) shows a streak-line visualization of this process. When the final interface between the last two cells breaks down the solute gradient is essentially destroyed. In a tank of finite height the background stratification is depleted by vertical transport of solute through the cells. If the tank had been infinitely tall it is possible that the cell size would have approached a stable equilibrium value with a vertical solute transport independent of time.

5. Conclusions

We have found theoretical and experimental evidence for a subcritical resonant instability of a flow with crossed isothermal and isosolutal lines. The physical nature of this resonant destabilization is intimately connected with the initial stabilization of perturbations by the very weakly diffusive vertical solute gradient. The energy of the perturbations ultimately comes from the differential heating. As the problem has been formulated, it would appear that they draw energy from the tilted solute distribution, but this is established in response to the heating. At later times, after a 'fracture' in the vertical solute gradient has established a height scale for the cells, the perturbations are driven thermally. This becomes increasingly evident as time goes on. The cells attain a boundary-

layer structure and after the solute has finally been homogenized there is a single thermally driven cell. The crucial question to which we have addressed ourselves in this paper is what governs the initial 'fracture' of the smooth solute distribution $S_0 \to z$. The resonant wavelength is that which allows the most efficient conversion of the basic available potential energy.

At second order the fundamental disturbance of wavenumber k modifies the horizontal basic fields in a sense that causes nonlinear stabilization (this is to be expected since the horizontal gradients provide the perturbation energy). The fundamental also modifies the vertically stabilizing solute gradient. The forcing term on the right-hand side of (3.7) demands a response to changes in solute caused by the fundamental motion. Since the diffusivity is small, the solute build-up essentially acts as a buoyancy driving force for the second-harmonic motion. However, the action of the second-harmonic motion reduces the basic stratification where the fundamental has vertical velocities, so that in fact the total disturbance can draw *more* energy from the available potential energy associated with the basic horizontal gradients. The phase and structure of the second-harmonic solute perturbation with respect to the fundamental vertical velocities is what determines whether or not there is subcritical instability. This is why the Landau constant changes sign across the resonance line; the second harmonic shifts phase by 180°. These statements can be made more clear if we consider the equation for the z-fluctuating solute variance. This can be obtained by multiplying (2.3) by S. We obtain

$$H\frac{\partial \frac{1}{2}S^2}{\partial t} = S\nabla^2 S - R_S wS - R_a H\left(uS\frac{\partial S}{\partial x} + wS\frac{\partial S}{\partial z}\right). \tag{5.1}$$

If we now substitute the interior expansions for u, w, S, t and R_a into (5.1) we shall obtain a sequence of solute energy equations. At the lowest order (ϵ) we obtain†

$$0 = S_1 \partial^2 S_1/\partial z^2 - R_S w_1 S_1 + R_{ac} H u_1 S_1. \tag{5.2}$$

This expresses the energy balance for the neutral solution as a sum of diffusional dissipation, eddy flux from the basic vertical gradient and eddy flux from the basic horizontal gradient. If we average this equation over a wavelength and across the gap by integrating, defining

$$\int_0^1 dx \int_0^\lambda dz \equiv \langle\ \rangle,$$

we find, after some integrations by parts and application of the approximate buoyancy equation (valid for $H \gtrsim |R_S|^{\frac{1}{6}}$) $\partial^4\psi/\partial z^4 = \partial S/\partial x$,

$$0 = -\left\langle\left(\frac{\partial S_1}{\partial z}\right)^2\right\rangle + R_S\left\langle\left(\frac{\partial^2 \psi_1}{\partial z^2}\right)^2\right\rangle + R_{ac} H\langle u_1 S_1\rangle. \tag{5.3}$$

The neutral wave is damped by diffusion and by the stable vertical density gradient and generated by eddy flux out of the basic horizontal gradient. In particular (5.3) requires that $\langle u_1 S_1\rangle > 0$, a fact which can be verified by direct computation.

The $O(\epsilon^{\frac{3}{2}})$ variance equation vanishes identically on application of the periodicity condition.

† Since we are considering only the interior flow ∇^2 becomes $\partial^2/\partial z^2$.

The $O(\epsilon^2)$ variance equation is

$$H\,\partial\langle\tfrac{1}{2}S_1^2\rangle/\partial\tau = \operatorname{sgn}(\epsilon)\,R_{ac}H\langle u_1 S_1\rangle - R_{ac}H\langle u_1 S_1 \bar{S}_{2x}\rangle - R_{ac}H\langle w_1 S_1 S_{2z} + u_1 S_1 S_{2x}\rangle. \quad (5.4)$$

The first term on the right-hand side represents the linear growth or decay. Since $\langle u_1 S_1\rangle > 0$, the sign of this term of course just depends on whether we are above or below the linear neutral curve. The second term is the usual nonlinear damping term which reflects the reduced eddy flux from the basic state because of the modification to the mean field by the interaction of the fundamental with itself. This term is always negative and usually serves to balance the first in a manner which establishes a steady equilibrium amplitude A_e. The third term is the one which is responsible for increasing $\langle\frac{1}{2}S_1^2\rangle$ even if ϵ is negative. Perhaps one interpretation of this term is that it represents eddy fluxes of solute from the harmonic to the fundamental. It is clear that the sign of this term will change as one crosses the k_r resonance line since u_1, w_1 and S_1 retain their signs but S_2 changes its sign. The computations of § 3 showed that subcritical instability was possible for $k < k_r$. By using the equation for conservation of S_2 it is possible to rewrite (5.4) as

$$H\,\partial\langle\tfrac{1}{2}S_1^2\rangle/\partial\tau = \operatorname{sgn}(\epsilon)\,R_{ac}H\langle u_1 S_1\rangle - R_{ac}H\langle u_1 S_1 \bar{S}_{2x}\rangle + \left\langle -\left(\frac{\partial S_2}{\partial z}\right)^2 + R_S\left(\frac{\partial^2\psi_2}{\partial z^2}\right)^2 + R_{ac}Hu_2 S_2\right\rangle,$$

which illustrates the perhaps obvious point that the ultimate energy source for subcritical instabilities is the total (fundamental + harmonic) eddy flux from the basic S_0 field. The subcritical instability process is connected with the boundaries since fundamental solutions in an infinite domain ($\propto e^{ik(z+ax)}$) do not generate a harmonic.

It is natural to ask if any other systems might exhibit similar effects. Veronis (1965) found finite amplitude instability in thermal convection between horizontal plates with a stabilizing solute gradient, but there the destabilization was a result of the mean correction; there are no harmonics. One wonders if the linear diffusive instabilities discussed by McIntyre (1970) might have finite amplitude destabilization if boundaries were included in the problem. This would mean that diffusive overturning could occur at larger stratification or smaller thermal winds than those needed for linear instability and hence the mechanism might become more relevant to geophysical fluid flows. The resonance instability mechanism may be present in other hydrodynamical stability problems where tilted fundamental cells generate (or are coupled to) higher harmonics. Apparently three-wave three-dimensional resonances are possible in supercritical Blasius flows (Raetz 1959; see also discussion in Stuart 1962), but to my knowledge the present work shows the first theoretical and experimental evidence of two-wave two-dimensional subcritical resonant instability.† However, such behaviour

† There is of course the well-known two-wave (self-resonant) capillary wave interaction, but this has not been posed as a stability problem (with energy flows to and from a mean state). If it were, there might well be similar effects. Certainly there is evidence that these capillary waves are unstable and that energy flows to longer wavelengths, as in wind generation of sea waves.

probably would not be discovered in perturbation analyses conducted near the critical point (R_{ac}, k_c).

In terms of the experiments it appears that the sideways diffusive instability mechanism is responsible for the initiation of layering, but by the time the cells have made transitions to vertical wavelengths of the order of the width of the box, there is a direct thermal driving of each cell with solute stabilized interfaces limiting the extent of the convection. Once the system has reached this level, it probably has much in common with the problem of an initial salt gradient heated from below, studied by Turner (1968). It will be interesting to study the detailed processes which lead to the breakdown of interfaces in our experiment.

The author would like to thank a referee for suggesting the use of equation (5.1) in the discussion of the instability mechanism. The laboratory and theoretical work described here was supported in part by N.S.F. grant GA-34937.

REFERENCES

BAINES, P. G. & GILL, A. E. 1969 On thermohaline convection with linear gradients. *J. Fluid Mech.* **37**, 289.

BAKER, D. J. 1966 A technique for the precise measurement of small fluid velocities. *J. Fluid Mech.* **26**, 273.

BAKER, D. J. 1971 Density gradients in a rotating stratified fluid: experimental evidence for a new instability. *Science*, **172**, 1029.

BLUMSACK, S. L. 1967 Formation of layers in a stably stratified fluid. *Geophys. Fluid Dyn. Summer Notes* II, *W.H.O.*, p. 1.

CHEN, C. F., BRIGGS, D. & WIRTZ, R. A. 1971 Stability of thermal convection in a salinity gradient due to lateral heating. *Int. J. Heat & Mass Transfer*, **14**, 57.

HART, J. E. 1971 On sideways diffusive instability. *J. Fluid Mech.* **49**, 279.

MCINTYRE, M. E. 1970 Diffusive destabilization of the baroclinic circular vortex. *Geophys. Fluid Dyn.* **1**, 19.

NIKOLAEV, B. I. & TUBIN, A. P. 1971 On the stability of convective motions of a binary mixture in a plane thermal diffusion column. *Prikl. Math. Mech.* **35**, 248.

OSTER, G. 1965 Density gradients. *Sci. Amer.* **213**, 70.

RAETZ, G. S. 1959 *Northrop Rep.* NOR-59-383 BLC-121. (See Stuart 1962.)

STERN, M. E. 1960 The salt fountain and thermohaline convection. *Tellus*, **12**, 172.

STUART, J. T. 1962 Nonlinear effects in hydrodynamic stability. *Proc. 10th Int. Congr. Appl. Mech.* p. 63. Elsevier.

THORPE, S. A., HUTT, P. K. & SOULSBY, R. 1969 The effect of horizontal gradients on thermohaline convection. *J. Fluid Mech.* **38**, 375.

TURNER, J. S. 1968 The behaviour of a stable salinity gradient heated from below. *J. Fluid Mech.* **33**, 183.

TURNER, J. S. & STOMMEL, H. 1964 A new case of convection in the presence of combined vertical salinity and temperature gradients. *Proc. U.S. Nat. Acad. Sci.* **52**, 49.

VERONIS, G. 1965 On finite amplitude instability in thermohaline convection, *J. Mar. Res.* **23**, 7.

VERONIS, G. 1968 Effects of a stabilizing gradient of solute on thermal convection. *J. Fluid Mech.* **34**, 315.

WIRTZ, R. A., BRIGGS, D. & CHEN, C. F. 1972 Physical and numerical experiments on layered convection in a density-stratified fluid. *Geophys. Fluid Dyn.* **3**, 265.

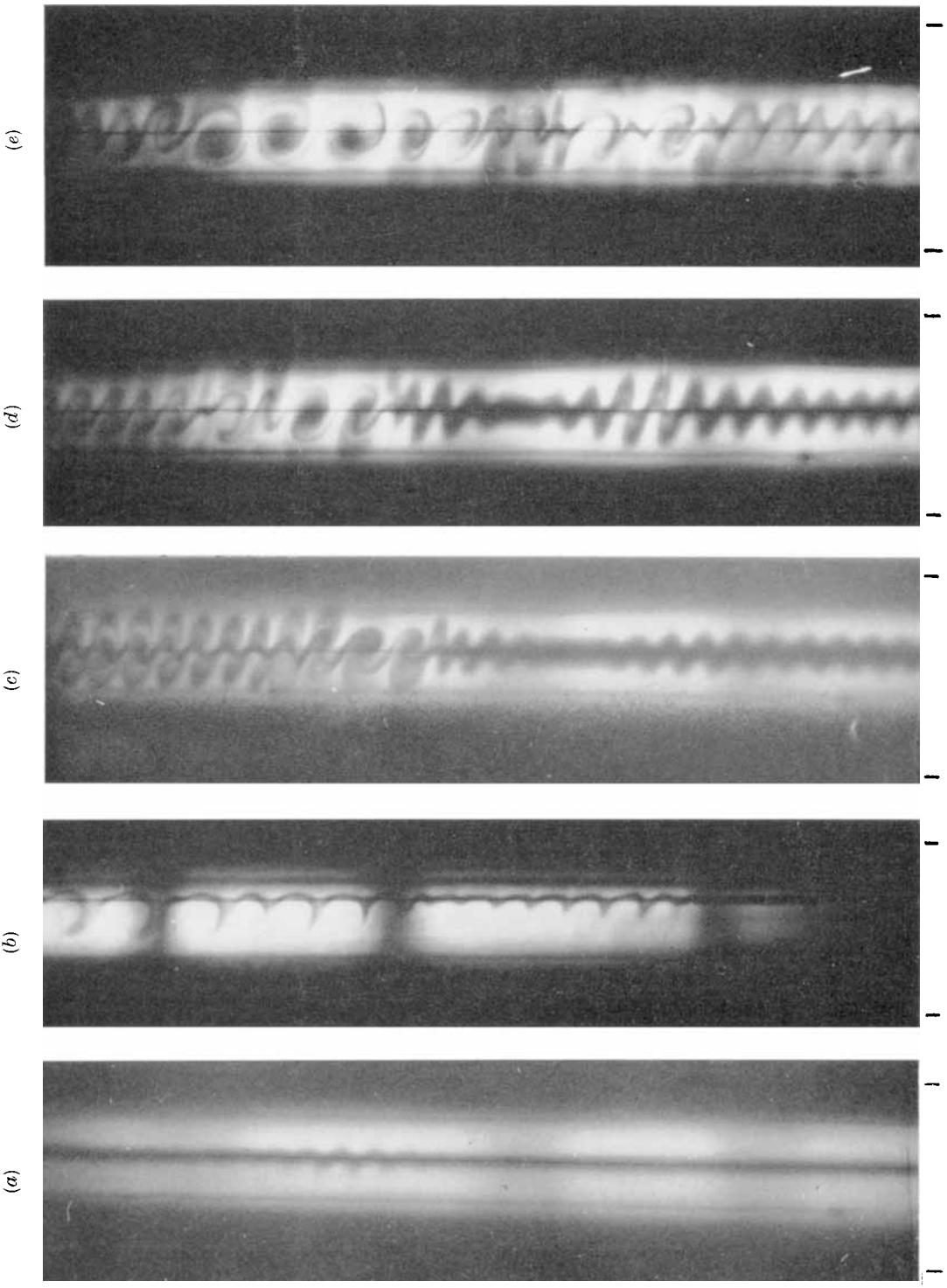

FIGURE 4. Visualization of the onset of waves and their subsequent development. $H = 281$, $P_r = 6{\cdot}7$, $R_S = -2{\cdot}74 \times 10^7$ and $R_a \doteq 2{\cdot}4 \times 10^4$. The time interval for the sequence (*a*), (*c*), (*d*), (*e*) is roughly 15 min. Figure 4(*b*) shows what the first disturbances look like when viewed from a dye wire located in the side-wall boundary layer.

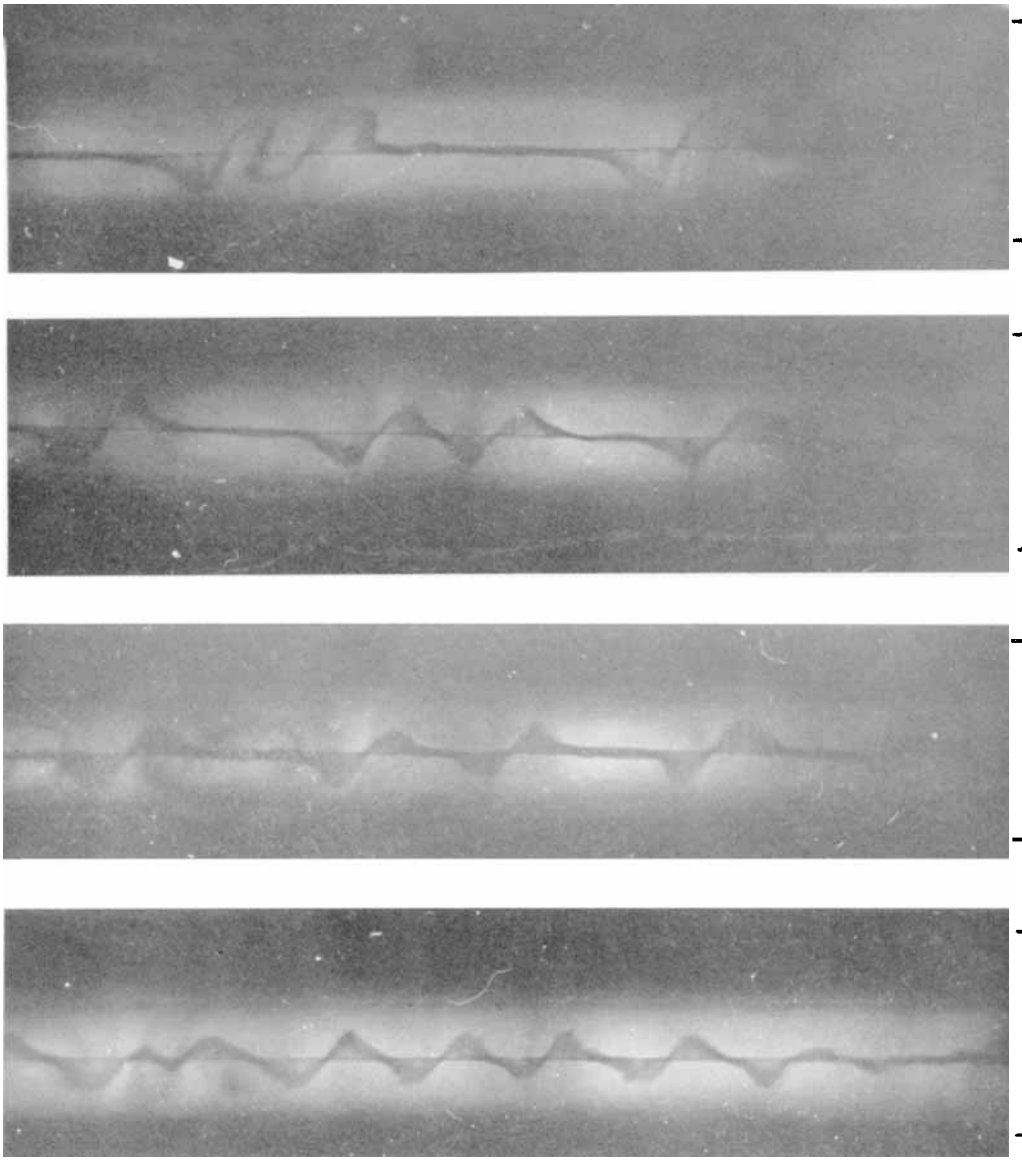

FIGURE 8. Dye-line observations of cell evolution. $R_S = -2{\cdot}74 \times 10^7$.

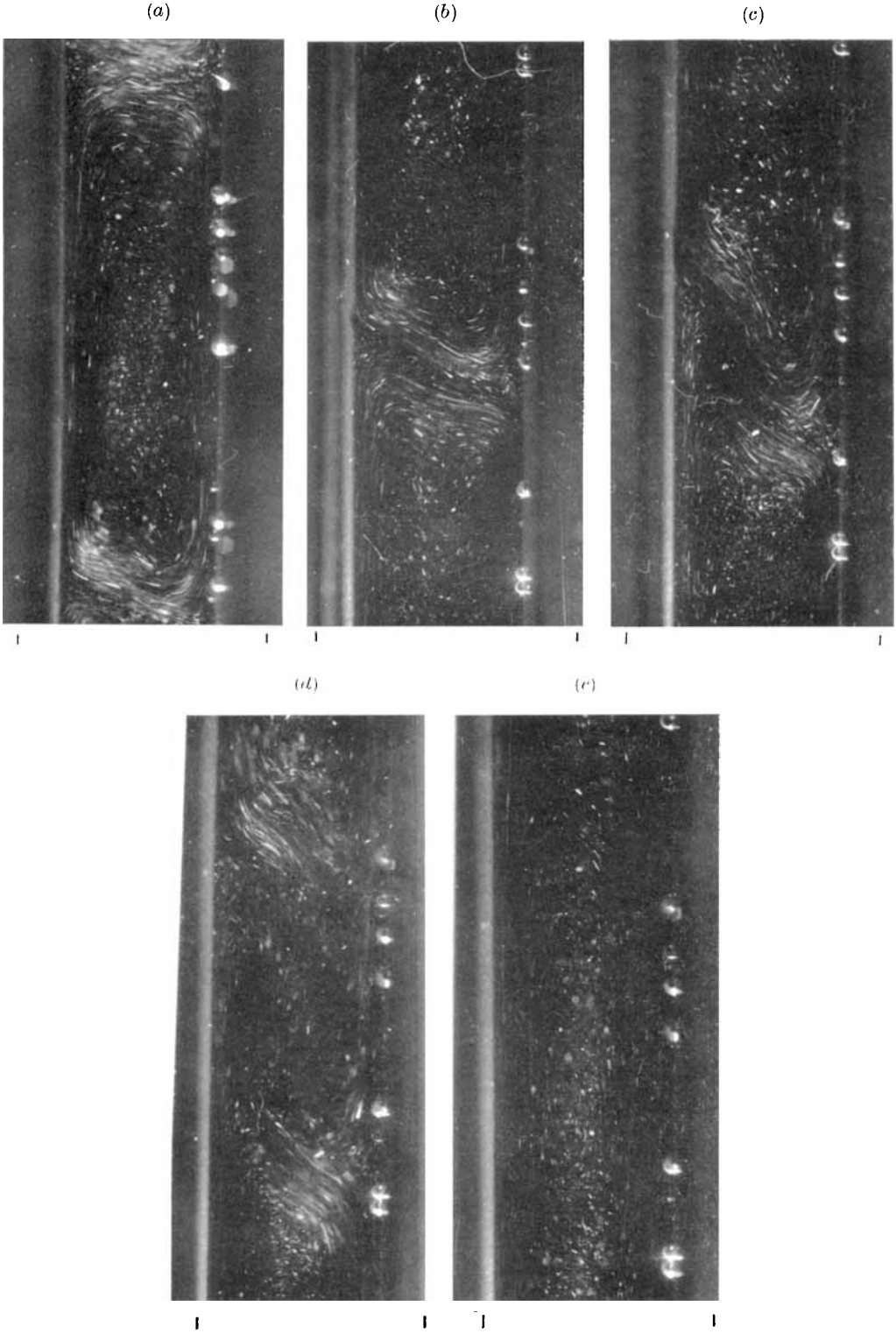

FIGURE 9. Breakdown of interfaces. (*a*) Typical cell at large ΔT or t. Note the boundary-layer structure. (*b*)–(*e*) Collapse of the interface. Note the steepening to a vertical position, breakdown (*d*) and establishment of a new cell. The time interval between (*b*) and (*e*) was about 5 min. The exposure time was 1 s.